PHYSICAL REVIEW B VOLUME 48, NUMBER 24 15 DECEMBER 1993-II

Nitrogen doping of highly tetrahedral amorphous carbon

V. S. Veerasamy
Engineering Department, University of Cambridge, Trumpington Street, Cambridge CB2 1PZ, United Kingdom

J. Yuan
Cavendish Laboratory, University of Cambridge, Madingley Road, Cambridge CB3 0HE, United Kingdom

G. A. J. Amaratunga and W. I. Milne
Engineering Department, University of Cambridge, Trumpington Street, Cambridge CB2 1PZ, United Kingdom

K. W. R. Gilkes
Cavendish Laboratory, University of Cambridge, Madingley Road, Cambridge CB3 0HE, United Kingdom

M. Weiler
Universität Kaiserslautern, Erwin Schrödinger Strasse, Kaiserslautern, Germany

L. M. Brown
Cavendish Laboratory, University of Cambridge, Madingley Road, Cambridge CB3 0HE, United Kingdom
(Received 11 August 1993)

Successful control of the conductivity of tetrahedrally bonded amorphous carbon (*ta*-C) by incorporation of N during film growth is reported. N is introduced into the films during growth by injecting N_2 gas into a plasma stream formed by a carbon cathodic vacuum arc. X-ray-photoemission-spectroscopy studies of films prepared over a range of N_2 partial pressures show that the N concentration varies from 2% to below the detection limit. Spectroscopic studies using electron-energy-loss spectroscopy confirm that the *ta*-C films with N contents up to 1 at. % retain their predominantly tetrahedral amorphous structure. The as-deposited *ta*-C, with no intentional N incorporation, is *p* type with a resistivity of 10^7 Ω cm and an activation energy of 0.22 eV. The addition of N under varying injection levels from 10^{-3} to 10 standard cubic cm causes the resistivity to initially go through a maximum at 10^9 Ω cm and then decrease monotonically to 10 Ω cm. A systematic variation of activation energies with increasing N_2 flow rate is observed, going through a maximum at about 1.0 eV before decreasing to 0.12 eV. The optical band pseudogap is shown to vary only marginally from the usual 2-eV benchmark. The properties of the doped film can be explained using a simple model of the electronic structure of the tetrahedral amorphous carbon.

I. INTRODUCTION

Thin films deposited from a filtered cathodic vacuum arc plasma show no detectable hydrogen and have remarkable properties of high density (≥ 3 g/cm^3), hardness, and Young's modulus.[1–4] Spectroscopic studies from electron-energy-loss spectroscopy (EELS) have shown that the films can contain up to 90% sp^3 diamond-like bonding within an optimized ion energy window 20–200 eV.[1,3–6] Neutron diffraction also confirms the tetrahedral nature of this material.[7–9] However, unlike Si, the C valence orbitals can hybridize to sp^3, sp^2, or sp configurations, giving rise to a tetrahedral, trigonal, or linear environment, respectively, around each atom. Robertson[2] has suggested that while the σ bonds control the physical properties giving this material its diamond-like character, the π states from trigonally bonded atoms contribute substantially to bandtailing, providing a plausible explanation for the small size of the observed pseudogap (2–2.2 eV) (Refs. 5 and 10) compared with the 5.5 eV indirect band gap of diamond.

Films of tetrahedral amorphous carbon (*ta*-C) are smooth and can be deposited at room temperature,[5] making them potentially useful for electronic applications. When considering the possible use of *ta*-C as a semiconductor, the controlled variation of conductivity through doping is of primary importance. In this respect, *ta*-C films are more useful than native *a*-Si films owing to a much lower density of dangling bonds. It has recently been shown that successful *n*-type doping of *ta*-C using phosphorus (up to 1%) is possible without changing its structure.[10] This result, coupled with the observation of a photoconductive effect,[11] makes the use of this material in semiconductor devices an interesting possibility. As P has a large atomic radius, doping by smaller N atoms would be preferable. In this paper we report the observation of significant changes in resistivity, activation energy, and thermopower with incorporation of N in *ta*-C. Based on optical, electrical, and structural properties we show that N does act as an effective *n*-type dopant below and up to a threshold of 1%. At higher concentrations of N (10%) the sp^2 component of both C and N increases dramatically, producing a C-N alloy.

0163-1829/93/48(24)/17954(6)/$06.00

II. EXPERIMENTAL METHOD

Thin films of *ta*-C were deposited from a compact filtered vacuum arc deposition system where a 99.999% purity high-density graphite cathode acts as the plasma source.[12,13] A toroidal 90° magnetic filter is used to remove macroparticles and neutrals from the plasma stream. N_2(99.9995% pure) is introduced into the vacuum chamber via a leak valve in the bend region. The N_2 partial pressure was monitored using an ion gauge and mass spectrometer assembly fitted to the deposition chamber unit. The pressure during deposition varied between 10^{-4} and 10^{-3} mbar and hence only the initial N_2 partial pressure and flow rate prior to arcing were used as the controllable parameter. The arc current and voltage used were 60 A and 20 V, respectively. The N_2 background partial pressures were varied from below 10^{-7} to 10^{-2} mbar. Dissociation and ionization of the background gas (N_2 in this case) are affected by the highly energetic ions and electrons from the plasma stream. Evidence for the presence of N^+ ions in the plasma was obtained from optical spectroscopic analysis which showed the most likely N $^2P \rightarrow {}^4S$ transition at 346.6 nm.[14] Highly reactive N^+ gas ions were thus incorporated into the growing films. The substrates were left at floating potential and their temperature never exceeded 80 °C during deposition.

Films with thicknesses ranging from 50 to 100 nm were grown on quartz and silicon (100) subtrates. Using a photoresist patterning and lift-off technique, each substrate was partly coated from the plasma stream so as to allow step measurements of film thickness using a Dek-Tak profilometer. Film thickness on silicon substrates was also estimated by ellipsometry. The N content in the films was determined using x-ray photoelectron spectroscopy (XPS) carried out on a Perkin Elmer ESCA system, model 5500, coupled with a spherical capacitor analyzer (SCA) with a pass energy set to 117.4 eV, giving an energy resolution of the order of $\Delta E = 2.3$ eV. The x-ray source was operated at 250 W (15 kV) using a Mg anode. The source was positioned at an angle of 54° with respect to the import lens axis of the analyzing system kept at a distance of 6 mm from the sample. The sample was positioned at an angle of 45° with respect to the lens axis and the area analyzed at a time was 0.8–1.2 mm^2. The data evaluation was carried out on the basis of empirical sensitivity factors taken to be 0.477 for N in the present system. The detection limit of this technique is 0.2 at. % N, which is sensitive enough for the detection of low levels of N ($<1\%$). Analysis of *ta*-C samples with no intentional leakage of N_2 gas yields concentrations of 99.9% C with traces of O and Ar. The traces of Ar are attributed to the sputter cleaning of the sample surface by Ar^+ bombardment prior to the XPS measurements. Within the partial pressure range of 10^{-7}–10^{-3} mbar, the lowest observable N concentration was 0.25% and the highest concentration of N was found to be about 1% (Fig. 1). The N content was below the level of detection in the *ta*-C film with no intentional introduction of N. The resistivities of the films were found to vary as a function of N_2 partial pressure and hence N content.

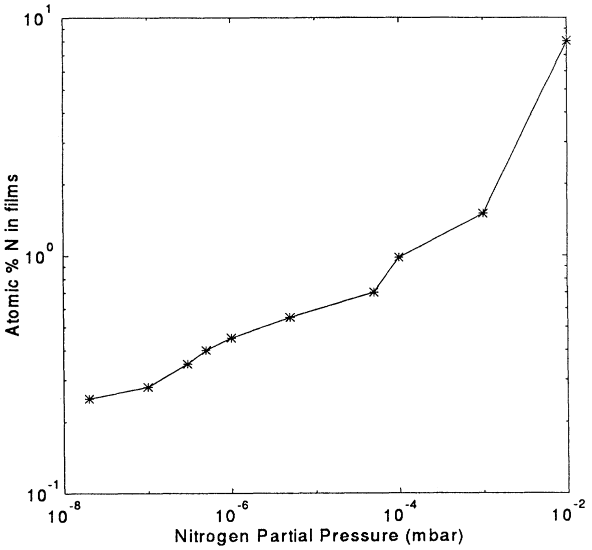

FIG. 1. Content of N in at. % in the films as a function of N_2 gas partial pressure.

III. ELECTRICAL PROPERTIES

Films deposited on quartz were used for both optical and electrical measurements. The electrical contacts were obtained by evaporating 100-nm-thick gold metal to form both gap cells (5 mm long × 0.5 mm gap width) and Van der Pauw-type structures[15] from which room-temperature resistivities were determined. The variation of film resistivity with N_2 partial pressure is shown in Fig. 1. Changes in resistivity as well as thermopower were also measured as a function of temperature over the range 180–500 K. The variation of electrical conductivity with temperature provides important information on the conduction mechanism in the bulk material. All films containing below and above 0.45% of N show a linear dependence in ln(conductivity) with reciprocal of thermodynamic temperature, indicative of thermally activated conduction. The gradient of the $\ln(\sigma)$ vs $(1/T)$ lines change with the differing N contents in the film. Ascribing these gradients over the range of temperature measured, to the corresponding activation energies E_a,[14] an increase in activation energy is first observed followed by a gradual decrease with increasing N partial pressures, as shown in Fig. 2(a). The film with the highest resistivity, containing 0.45% N, displayed a linear relationship between $\ln(\sigma)$ and $T^{-1/4}$ over a wide temperature range, characteristic of variable-range hopping.

In amorphous semiconductors, thermopower measurements are essential to determine whether doping has been achieved and, if it has, whether the carriers are electrons or holes. From our results there is a clear change in the sign of the thermopower from positive to negative in the case of undoped films compared to films containing 2% N. In the latter films the order of magnitude of thermopower values (in the mV/K range) suggests a conduction mechanism involving electrons thermally activated into the conduction band, corresponding to regular *n*-type doping. In the case of undoped films the thermopower is positive and of the order of 0.1 mV/K indicating that conduction takes place via valence-band extended states. In the film with the highest resistivity (0.45% N; N_2 partial pressure 1×10^{-6} mbar) the thermopower is in the μV/K regime which suggests a conduction mechanism around the Fermi level and correlates with the variable-range-hopping-type mechanism suggested by the $T^{1/4}$ dependence discussed above.

The *p*-type behavior of undoped *ta*-C films with an activation energy 0.2–0.22 eV (Refs. 5 and 10) is thought to be due to some structural defect in the carbon network. The observation that with increasing N content, a gradual rise in both activation energy and resistivity to a maximum value followed by a decrease leads to the following interpretation: The Fermi level moves from being close (~0.2 eV) to the valence band towards the midgap region with the initial incorporation of N. Further increase of N content shifts the Fermi level towards the conduction band which manifests itself as a reduction in activation energy and resistivity. The N atom first compensates for the defect-controlled *p*-type material and subsequently dopes it *n* type. This result confirms the inference made from space-charge-limited-current (SCLC) flow studies[16] that the density of states in undoped *ta*-C is low enough to yield an unpinned Fermi level. The unpaired dangling-bond density obtained from electron-spin resonance (ESR) measurements for undoped *ta*-C is of the order of 10^{18}–10^{19} cm^{-3}.[16] This value is two orders of magnitude lower than in other unhydrogenated amorphous group-IV elements.

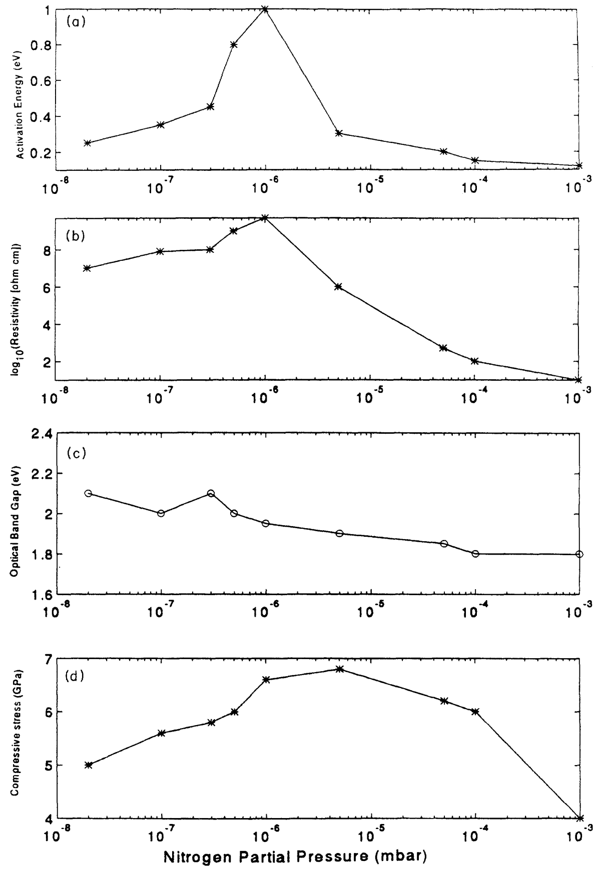

FIG. 2. Variation of (a) activation energy, (b) electrical resistivity, (c) Tauc optical gap, and (d) compressive stress with N_2 partial pressure.

IV. OPTICAL PROPERTIES

The optical band gap E_g was determined for films grown under similar conditions on quartz substrates. The corresponding absorption coefficients of the thin films in the range of 30–50 nm were measured in the wavelength range 190–750 nm. E_g was determined using a Tauc plot, the usual procedure for amorphous materials.[17] The variation of E_g with N content is shown in Fig. 2(c). Thus within the limits of experimental error the optical band gap decreases slightly to 1.8 eV with up to 1.5% N. With 10% N incorporation, the optical band gap reduces to 1.5 eV. Using the reflectance and transmission of the *ta*-C films the real and the imaginary parts of the refractive index have also been extracted. This allows for the subsequent calculation of the imaginary permittivity ε_{20} of *ta*-C. The optical data are compared with the EELS data in the next section.

V. EELS STUDY OF N-DOPED *ta*-C FILMS

In order to further establish clearly whether chemical doping has taken place, a comparative study of *ta*-C films with and without doping was made using EELS. This was performed on a Vacuum Generators (VG) HB501 scanning transmission electron microscope coupled with a dedicated parallel EELS spectrometer.[18,19] Thin films grown on silicon were lifted off using a mixture of HF, HNO_3, and acetic acid. Each set of films was placed on electron microscope support grids. The typical resolution of the spectra was 0.5 eV. The energy-loss spectra of the valence excitation as well as the C *K* edges were collected with a focused probe scanning over a large area so as to average over any possible composition fluctuations. The convergence angle of the electron probe was 5 mrad and the spectrometer collector subtends a semiangle of 7 mrad. With a total beam current of the order of 10^{-9} A and a defocused probe, no sign of radiation-induced change in the energy-loss spectra was observed. Thus we are confident that the results obtained are intrinsic to the samples under investigation. Four samples were examined, the first undoped, the rest containing 0.5%, 1%, and 10% N, respectively. The first three samples cover the entire range of N concentrations where controlled doping has been achieved.

The C *K*-edge spectra of these *ta*-C films are shown in Fig. 3 where they have been deconvoluted with the valence electron spectra obtained from the same area to remove both the multiple scattering contribution as well as the effect of instrumental response profile. As is known from earlier work on such films,[6,7] the C *K* edge consists of a pre-edge structure plus a broad background. Within the dipole transition limit, the pre-edge peak is attributed to the transition from $1s\rightarrow 2p(\pi^*)$ in C atoms

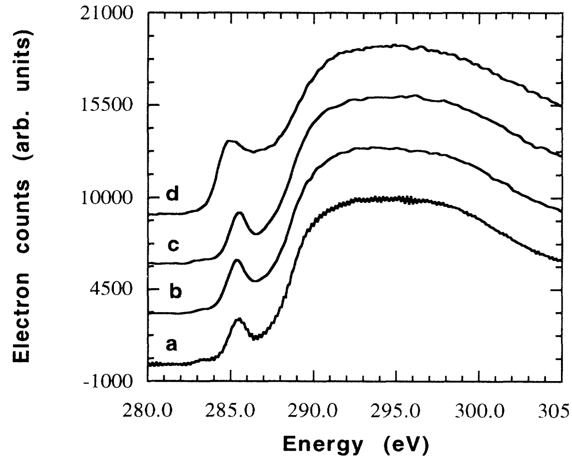

FIG. 3. The C *K*-edge spectra from the undoped *ta*-C film (a) and from the *ta*-C films with 0.45% (b), 1% (c), and 10% (d) nitrogen levels.

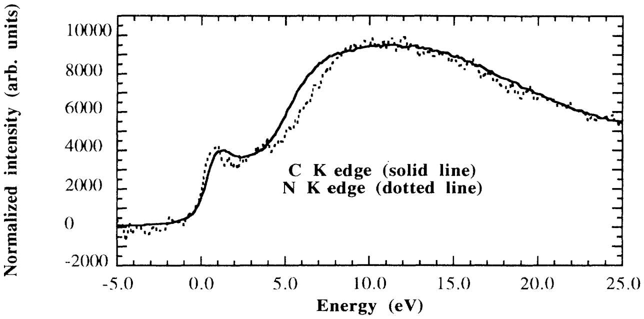

FIG. 4. A comparison of the C *K* edge and the N *K* edge from a 10% N-doped vacuum arc deposited carbon film. The spectra have been processed to subtract the background and aligned at the leading edge of the pre-edge peaks.

with non-sp^3 bonding configuration, and the broad peak is attributed to the $1s \rightarrow 2p(\sigma^*)$ transition in C atoms. Various schemes have been proposed to calculate the sp^2 fraction in this material.[3,6] However, in this work only a comparative study is made between the undoped films and N-doped films. For the 0.5% N sample, both the pre-edge as well as the shape of the broad peak are very similar to that of the undoped film. In the case of the 1% N-doped sample, the shape of the pre-edge peak remains unchanged within the experimental error, but the main absorption peak centered around 292 eV becomes broadened. After taking into account the latter observation, the area under the $1s \rightarrow 2p(\pi^*)$ peak is constant, indicating that the effect of the N doping on the film at this level is minimal and local as far as the sp^2/sp^3 fraction is concerned. The broadening of the peak at 292 eV with N doping up to 1% N could therefore be attributed to an increased range of disorder in the σ-bonded structure, instead of a growth of the fraction of sp^2 bonds.

The C *K*-edge spectrum in the case of the sample containing 10% N shows a very different fine structure from the others. The pre-edge peak is not only increased in intensity, but its position is also shifted to a lower energy by 0.5 eV and becomes broadened. This suggests that excessive N doping promotes a disordered sp^2 structure. Another noteworthy feature is that the N *K* edge shows a structure similar to that of the C *K* edge (Fig. 4), indicating that the N atoms do not appear exclusively as either sp^2 or sp^3 bonded sites but rather on average sample the same local environment as that of the C atoms. Small differences do appear, however, in the fine structure of the C and N *K* edge, but this probably reflects atomic differences between N and C. The net role of N is consistent with the fact that the increase in the fraction of sp^2-bonded C is much higher than the increase in N concentration.

The valence electron-energy-loss functions of the samples were obtained from the raw spectra after correcting for the zero-loss profile and for the aperture function together with the removal of the multiple scattering contribution. They are compared with the optically derived energy-loss function to verify the validity of the pseudogap determination by the Tauc method since the extrapolation to the optical gap does depend on the accuracy of the dielectric function in the far ultraviolet region. To achieve this comparison, the experimental energy-loss function has been scaled with the optically derived energy-loss function [Fig. 5(a)]. The agreement is excellent, both for the doped material as well as the undoped material for energies up to 4.5 eV. Above this energy, the difference may be attributable to the difficulty of optical measurement in the uv region. However, the band-gap determination is not affected by using only data below 4.5 eV. Direct determination of the optical band gap from EELS, by visual examination, is not easy because of the lack of a Van Hove–type singularity associated with the band gap in crystalline materials. Nevertheless, the sudden drop in the energy-loss intensity [Fig. 5(b)] around 2 eV in the undoped as well as the 0.5% and 1% doped material corroborates with the conclusion from the optical Tauc plot that the band gap is of the order of 2 eV.

The valence electron plasmon energies of the 1% doped and undoped material are different by less than 0.5 eV at about 30 eV. This indicates the negligible change in electronic density and hence the sp^2/sp^3 ratio. In contrast, the valence electron plasmon energy drops to 27 eV for the 10% N-doped sample, consistent with an increase in the low density sp^2 component.

VI. COMPRESSIVE STRESS

The compressive stress in the films has been identified to be an important parameter which is strongly correlated with the sp^3 bonding in the material. The investigation of stress with differing N_2 partial pressures and hence flow rate has therefore been determined. The measurements have been made for three independent runs over the same range of N_2 partial pressures. The stress in the films has been calculated using a method in which the curvature of the silicon {100} substrate is measured prior to and after deposition using a DekTak 3030 stylus profilometer.[3] The subsequent use of Stoney's equation allows calculation of the film stress.[4] The stress is maintained and interestingly rises initially with increasing gas flow rate, and then at higher flow rate starts to decrease [Fig. 2(d)].

We conclude that the sp^3 fraction in the films is preserved with low N incorporation. The reason for a decrease in stress at high pressures of N is twofold: a reduction in the energy of the incident C ions[3] in collision with N_2 gas or the incorporation of a high level of N causes stress relaxation. A control experiment with argon gas was also performed and showed a monotonic decrease in stress with increasing Ar_2 gas pressure, implying that the initial increase in stress in N-doped films is due to the incorporation of N.

VII. DISCUSSION

The structure of N-doped *ta*-C is seen to have two phases. In the lightly doped region the structure remains highly tetrahedral although more disordered. Above a certain dopant level (5%–10%) a predominantly trigonal C-N alloy is formed. This may be understood within the following scheme: the metastability of the tetrahedrally bonded *a*-C and crystalline diamond hinges on the energy barrier that prevents the relaxation of sp^3 bonded C atoms to sp^2 configuration. Arguments using constraint theory predict that a predominantly tetrahedral amorphous structure will be overconstrained, i.e., the sp^3 hybrid orbitals which deviate from their ideal orientation in forming an sp^3 network, resulting in a highly strained structure. This picture is consistent with neutron scattering results[7–9] which show a small difference between the bond length of *ta*-C and crystalline diamond, but a significant spread in the bond angle. The large compressive stress measured from as-grown samples for the undoped material is testament to the presence of a large energy barrier for the angular deviation of sp^3 from the ideal orientation. The introduction of N is expected to change this energy barrier either by introducing a polar component into the sp^3 orbitals or by doping the sp^3 orbital, or a combination of both. Since the undoped material exhibits *p*-type behavior, it is expected that the filling of the hole states will slightly increase the energy cost of bond angle disorder and the additional doping by the electron in the antibonding states of the sp^3 will reduce this energy cost. Thus the compressive stress in the material for a given amorphous structure is expected to rise first then decrease. This is clearly the case for N incorporation where the stress first increases from 5 to 8 GPa before falling off to 4 GPa at a N concentration of 1%. One consequence of the reduced energy cost will be greater structural disorder in the heavily doped films, which could be checked by a careful neutron scattering experiment. However, the increased width of the $1s \rightarrow 2p(\sigma^*)$ energy-loss peak may be interpreted as a consequence of such additional disorder. Excess N dopant will reduce the energy barrier for sp^3 to sp^2 transition to such a small value that graphitization can proceed around the N atom. This is consistent with the recent observation[18] of increased sensitivity of the sample for radiation-induced graphitization in doped samples.

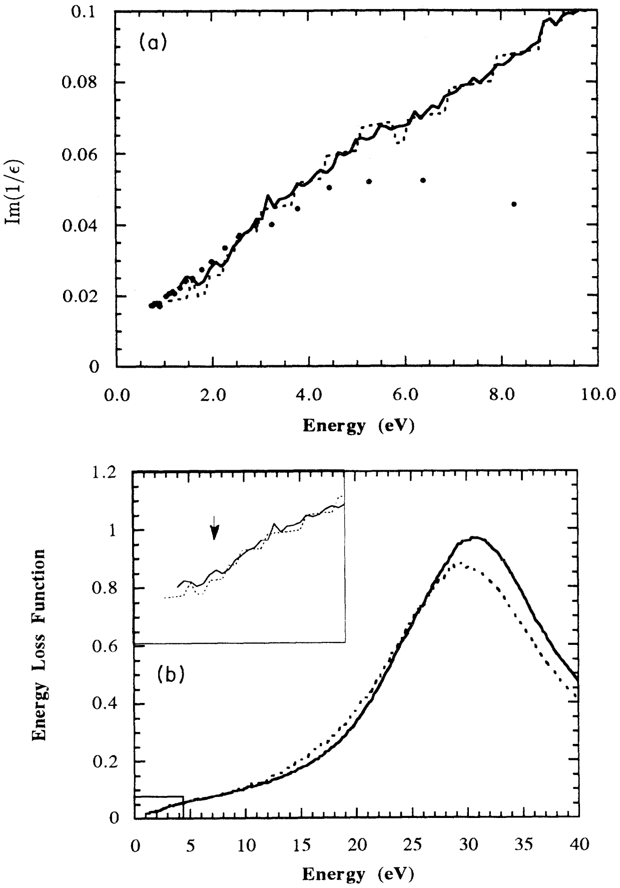

FIG. 5. (a) Comparison of the optically derived electron-energy-loss function (points) with the experimentally determined electron-energy-loss function for both undoped *ta*-C film as well as 1% N-doped *ta*-C films. (b) The electron-energy-loss functions of undoped (solid line) and 1% N-doped *ta*-C film (dashed line). The low-energy region is magnified as an inset. (The position of a possible optical gap is indicated by the arrow.)

The experimental observation enables interpretation of the electronic structure of N-doped *ta*-C. The *p*-type conductivity in the undoped material may be due to some defect in the network, perhaps fivefold-coordinated carbon. The resulting holes are filled by "substitutional" doping of the N atom, moving the Fermi level upwards in the tail state of the valence band. The shift in the Fermi level raises the activation energy for hole conduction. When the Fermi level is in the middle of the gap the density of states is low and electrical conduction is by variable-range hopping. Further doping raises the Fermi level beyond the half-filled state and electronic transitions are made by the thermally excited carriers in the extended states of the conduction band. The high-energy position of the $1s \rightarrow 2p(\pi^*)$ peak and its narrow width would suggest that the cluster sizes are small and isolated. Its relative insensitivity to low-level N doping indicates that at that level N predominantly enters the sp^3-bonded region.

However, in *ta*-C, unlike diamond, there is a significant fraction of sp^2 estimated to be 20±10%. The $\pi \rightarrow \pi^*$ transitions associated with the sp^2 bonds determine the 2-eV optical gap of *ta*-C (in diamond the $\sigma \rightarrow \sigma^*$ transitions control the 5.5-eV band gap). Therefore it is possible that with increasing N concentration a significant fraction of the N bonds to the sp^2 carbon. The actual electronic doping of the material and the consequent drop in resistivity with increasing N could therefore be associated with activation of a donor electron from the N into the π^* bands which forms a tail to the σ^* band. This would partially explain why N, which is a deep donor (1.5 eV below conduction band) in diamond, seems to act as a shallow *n*-type donor in *ta*-C. This view of electronic doping would require the π states to be delocalized so that extended state conduction can occur [as suggested by the $1/T$ dependence of $\ln(\sigma)$]. Whether 20% sp^2 is sufficient to give delocalized bandlike behavior by π-π^* states remains to be verified through theoretical simulation.

At 10% N or higher, a disordered C-N alloy is formed in which essentially trigonal bonds predominate. This results in a broadening of the π and π^* bands and the $\pi \rightarrow \pi^*$ transitions. This contributes to the eventual narrowing, but not the disappearance, of the band gap. The shift to a lower energy of the $1s \rightarrow \pi^*$ peak in the C-N alloy would increase the density of states in the vicinity of the Fermi level, resulting in a semimetallic material which is quite distinct from *ta*-C and N-doped *ta*-C. If a similar sp^2 type of hybridization is simultaneously maintained for both C and N atoms as the N ratio is increased, the likelihood of the formation of a C-N alloy with a β Si_3N_4 type of structure is remote; the reason being that such a structure would require the coexistence of both tetrahedral C and trigonal N.[21]

VIII. CONCLUSION

In this paper nitrogenation of *ta*-C has been studied in an attempt to achieve chemical doping. It is shown that incorporation of up to 1% N does not substantially alter the dominant tetrahedral structure of *ta*-C. The optical band gap is preserved within the nominal 1.9–2.0 eV range. However, the effect of N incorporation on the electrical properties of the material is dramatic. The resistivity is found to increase in the initial stages to a maximum and to then gradually decrease at above 0.5% N. The activation energy for electrical conduction varies accordingly, suggesting that the Fermi level in this material moves relative to the valence-band edge across the gap towards the conduction-band edge. Evidence of a change in the sign of the thermopower coefficient from positive to negative suggests that this wide-band-gap amorphous semiconductor is being progressively changed from *p* type to *n* type with increasing N concentration. We conclude that *n*-type doping of *ta*-C is possible with the incorporation of N to a level of 1%. Above that level, although the similarity in both the C and N *K* edges suggests that N incorporation is still largely substitutional, N predisposes the tetrahedral network to revert to an sp^2 phase.

---

[1] J. Koskinen, J. Appl. Phys. **63**, 2094 (1988).

[2] J. Robertson, Philos. Trans. R. Soc. London, Ser. A **342**, 277 (1993).

[3] P. Fallon, V. S. Veerasamy, C. A. Davis, J. Robertson, G. A. J. Amaratunga, W. I. Milne, and J. Koskinen, Phys. Rev. B **48**, 4777 (1993).

[4] D. R. McKenzie, D. Muller, and B. A. Pailthorpe, Phys. Rev. Lett. **67**, 773 (1991).

[5] V. S. Veerasamy, G. A. J. Amaratunga, W. I. Milne, P. Hewitt, P. J. Fallon, D. R. McKenzie, and C. A. Davis, Diamond Relat. Mater. **2**, 782 (1993).

[6] S. D. Berger, D. R. McKenzie, and P. J. Martin, Philos. Mag. Lett. **57**, 285 (1988).

[7] P. H. Gaskell, A. Saeed, P. Chieux, and D. R. McKenzie, J. Non-Cryst. Solids **150**, 126 (1992).

[8] P. H. Gaskell, A. Saeed, P. Chieux, and D. R. McKenzie, Philos. Mag. B **66**, 155 (1992).

[9] P. H. Gaskell, A. Saeed, P. Chieux, and D. R. McKenzie, Phys. Rev. Lett. **67**, 1286 (1991).

[10] V. S. Veerasamy, G. A. J. Amaratunga, C. A. Davis, A. E. Timbs, W. I. Milne, and D. R. McKenzie, J. Phys. Condens. Matter **5**, 169 (1993).

[11] G. A. J. Amaratunga, V. S. Veerasamy, W. I. Milne, C. A. Davis, and H. S. Mackenzie, Appl. Phys. Lett. **63**, 370 (1993).

[12] V. S. Veerasamy, G. A. J. Amaratunga, and W. I. Milne, IEEE Trans. Plasma Sci. **21**, 322 (1993).

[13] I. I. Askenov, S. I. Vakula, V. G. Padalka, V. E. Strel'nitski, and V. M. Khoroshikh, Zh. Tekh. Fiz. **50**, 2000 (1980) [Sov. Phys. Tech. Phys. **25**, 1664 (1980)].

[14] A. Wright and C. Winkle, *Active Nitrogen* (Academic, New York, 1964).

[15] L. J. Van der Pauw, Phillip Research Report (N. V. Philips, Eindhoven, The Netherlands, 1958), Vol. 13, No. 1, pp. 1–9.

[16] V. S. Veerasamy, G. A. J. Amaratunga, C. A. Davis, W. I. Milne, P. Hewitt, and M. Weiler, Solid-State Electron. (to be published).

[17] N. Mott and E. A. Davis, *Electronic Conduction in Non-Crystalline Materials,* 2nd ed. (Clarendon, Oxford, 1979).

[18] D. McMullan, J. M. Rodenburg, Y. Murooka, and A. J. McGibbon, in EMAG-MICRO 89, *Proceedings of the Institute of Physics Electron Microscopy and Analysis Group and Royal Microscopical Society Conference, London, September 1989,* edited by P. J. Goodhew and H. Y. Elder, IOP Conf. Proc. No. 98 (Institute of Physics and Physical Society, London, 1991), pp. 55–58.

[19] J. Yuan, A. Saeed, L. M. Brown, and P. H. Gaskell, Philos. Mag. B **66**, 187 (1992).

[20] C. A. Davis, D. R. McKenzie, Y. Yin, E. Kravtchinskaia, G. A. J. Amaratunga, and V. S. Veerasamy, Philos. Mag. B (to be published).

[21] A. Y. Liu and M. L. Cohen, Phys. Rev. B **41**, 10 727 (1990).